ISSN 1070-3284, Russian Journal of Coordination Chemistry, 2014, Vol. 40, No. 1, pp. 54–62. © Pleiades Publishing, Ltd., 2014.

Copper(II), Zinc(II), and Cadmium(II) Coordination Polymers with 2-Methylglutarato and 4,4'-Dipyridyldisulfide[1]

H. L. Zhu, J. Zhang, F.-Y. Yao, and Y.-Q. Zheng*

Crystal Engineering Division, Center of Applied Solid State Chemistry Research Ningbo University, Ningbo, 315211 P.R. China

**e-mail: yqzhengmc@163.com*

Received May 21, 2012

Abstract—Three new coordination polymers of copper(II), zinc(II) and cadmium(II), $Cu(H_2O)$(Dpds)(2-MGA) (**I**), [Zn(Dpds)(2-MGA)] · $1.25H_2O$ (**II**) and [$Cd(H_2O)$(Dpds)(2-MGA)] · $0.25H_2O$ (**III**) (Dpds = 4,4'-dipyridyldisulfide, H_2MGA = (*RS*)-2-methyl glutaric acid), have been synthesized and characteried by X-ray single crystal structure determination. The Cu atoms in **I** are alternately bridged by Dpds ligands and 2-methylglutarato ligands to generate 1D chain. The resulted chains are assembled via S···S weak interactions into 2D layers, which are through twofold 2D parallel/2D parallel mode inclined interpenetration to induce 3D supramolecular architecture. In **II**, the ZnN_2O_2 tetrahedras are bridged by 2-MGA anion and Dpds ligands to form 2D (4,4) networks, which are assembled via hydrogen bonds to 3D supramolecular architecture. The centrosymmetric binuclear units Cd_2(2-MGA)$_2$ in **III** are bridged by Dpds ligands to form 1D repeated rhomboids chains, which are interlinked via S···S weak interactions into 2D layer, and the resulting 2D sheets are inclined parallel into 3D network.

DOI: 10.1134/S1070328414010114

INTRODUCTON

There is currently significant interest in the design and synthesis of coordination polymer complexes due to their potential use as functional materials [1–4]. The generation of coordination polymers depends mainly on the combination of two factors, the coordination of the metal ions and the nature of the ligands. Thus, the most effective strategies are the judicious choices of special inorganic building blocks and organic linkers [5, 6]. Coordination polymers with rigid linear ligands, such as 4,4'-bipyridine and its derivatives have been well documented, but using twisted ligands like 4,4'-dipyridyldisulfide (Dpds) ligand could function more as a bridging ligand capable to form diverse and abundant dimensional architecture [7–11]. Dpds ligand shows a characteristic twisted structure with a C–S–S–C torsion angle of approximately 90° [7]. Furthermore, the sulfur atoms have additional coordination ability as well as the ability to accept hydrogen bonds or to establish other van der Waals interactions. In the designed synthesis of coordination polymers, the linear α,ω-dicarboxylic acid has been well explored [12–15], which can bridge metal centers to form a variety of coordination polymers ranging from 1D chains through 2D layers to 3D networks. Compared to linear α,ω-dicarboxylic acid, the branched α,ω-dicarboxylic acid, such as 2-methyl glutaric acid, has been seldom used to constructed coordination polymers [16–18]. In our course of ongoing study of the extended structural motifs based on (*RS*)-2-methyl glutaric acid (H_2MGA), we present herein three coordination polymers produced from 4,4'-dipyridyldisulfide and (*RS*)-2-methyl glutaric acid with Cu^{2+} or Zn^{2+} or Cd^{2+} $Cu(H_2O)$(Dpds)(2-MGA) (**I**), [Zn(Dpds)(2-MGA)] · $1.25H_2O$ (**II**), and [$Cd(H_2O)$(Dpds)(2-MGA)] · $0.25H_2O$ (**III**).

EXPERIMENTAL

Materials and physical methods. All chemicals of reagent grade were commercially available and used without further purification. Powder X-ray diffraction measurements were carried out with a Bruker D8 Focus X-ray diffractometer to check the phase purity. The C, H, and N microanalyses were performed with a PE 2400II CHNO/S elemental analyzer. The FT–IR spectra were recorded from KBr pellets in the range 4000–400 cm^{-1} on a Shimadzu FTIR-8900 spectrometer. Single crystal X-ray diffraction data were collected by Rigaku R-Axis Rapid IP X-ray diffractometer. The temperature-dependent magnetic susceptibilities were determined with a Quantum Design SQUID magnetomer (Quantum Design Model MPMS-7) in the temperature range 2–300 K with an applied field of 2 KOe.

Synthesis of I. Addition of 0.5 mL (1.0 M) NaOH to an aqueous solution of 0.063 g (0.25 mmol) $Cu(NO_3)_2 \cdot 3H_2O$ in 4.0 mL H_2O produced blue precipitate, which was separated by centrifugation, washed with distilled water for several times and then transferred into aqueous solution (at 80°C) of 0.073 g (0.5 mmol) 2-MGA and 0.051 g (0.25 mmol) Dpds in

[1] The article is published in the original.

30.0 mL water. The resulting mixture was further stirred for 30 min and insoluble solid was filtered off. The pale blue filtrate was kept still at 50°C in a constant temperature incubator and blue block crystals were formed in one week (the yield was 11.5% based on the initial $Cu(NO_3)_2 \cdot 3H_2O$ input). The phase purity of the product was checked according to powder X-ray diffraction patterns compared with the simulated PXRD based on the single crystal data.

For $C_{16}H_{17}N_2O_5S_2Cu$

anal. calcd., %:	C, 43.19;	H, 3.85;	N, 6.29;	S, 14.41.
Found, %:	C, 43.63;	H, 4.18;	N, 6.01;	S, 14.17.

IR data (KBr; ν, cm^{-1}): 3165 m, 3048 w, 2962 w, 2915 w, 1608 s, 1581 s, 1481 m, 1416 s, 1388 s, 1362 w, 1340 w, 1316 w, 1284 w, 1218 w, 1066 m, 818 m, 716 m, 701 m, 606 w, 494 w.

Synthesis of II. 0.5 mL (1.0 M) NaOH solution was slowly added to a mixture of 0.074 g (0.25 mmol) $Zn(NO_3)_2 \cdot 6H_2O$, 0.037 g (0.25 mmol) 2-MGA, 0.055 g (0.25 mmol) Dpds and 16 mL H_2O and stirred for 30 min in air. The mixture was then transferred to a 23 mL Teflon reactor and kept at 130°C for 5 h under autogenous pressure. After cooling to room temperature, the insoluble solid was filtered out and the filtrate was allowed at 50°C in a constant temperature incubator and colorless crystals were found in 3 days (the yield was 21% based on the initial $Zn(NO_3)_2 \cdot 6H_2O$ input).

For $C_{16}H_{18.5}N_2O_{5.25}S_2Zn$

anal. calcd., %:	C, 42.49;	H, 4.12;	N, 6.19.
Found, %:	C, 42.72;	H, 4.63;	N, 5.67.

The crystals of compound **II** were found to be unstable in air, so that no further characteriazaion was presented.

Synthesis of III. A similar method to that used for the preparation of **I** was followed for the preparation of **III** by replacing $Cu(NO_3)_2 \cdot 3H_2O$ with 0.066 g (0.25 mmol) $Cd(Ac)_2 \cdot 2H_2O$. Slow evaporation of the solution for one weeks at 50°C in a constant temperature incubator afforded colorless block-like crystals of **III** (the yield was 18% based on the initial $Cd(Ac)_2 \cdot 2H_2O$ input). The phase purity of the products were respectively checked according to powder X-ray diffraction patterns compared with the simulated PXRD based on the single crystal data.

For $C_{16}H_{16.5}N_2O_{5.25}S_2Cd$

anal. calcd., %:	C, 38.64;	H, 3.34;	N, 5.63;	S, 12.89.
Found, %:	C, 38.85;	H, 3.56;	N, 5.49;	S, 12.73.

IR data (KBr; ν, cm^{-1}): 3383 m, 3058 w, 2966 w, 2916 w, 1578 v. s, 1480 m, 1410 s, 1319 w, 1218 m, 1097 w, 1065 m, 816 m, 710 s, 490 m.

X-ray crystallography. Suitable single crystals were selected under a polarizing microscope and fixed with epoxy cement on respective fine glass fibers which were then mounted on a Rigaku R-Axis Rapid IP X-ray diffractometer with graphite-monochromated MoK_α radiation (λ = 0.71073 Å) for cell determination and subsequent data collection. The reflection intensities in suitable θ ranges were collected at 293 K using the ω–2θ scan technique. The employed single crystals exhibit no detectable decay during the data collection. The data were corrected for *Lp* and empirical absorption effects. The SHELXS-97 and SHELXL-97 programs [19] were used for structure solution and refinement. The structure were solved by using direct methods. Subsequent difference Fourier syntheses enabled all non-hydrogen atoms to be located. After several cycles of refinement, all hydrogen atoms associated with carbon atoms were geometrically generated, and the rest hydrogen atoms were located from the successive difference Fourier syntheses, while the water H atoms of split oxygen atom O(3) and O(4) in **II** could not be positioned reliably and were omitted from a difference Fourier map. Finally, all non-hydrogen atoms were refined with anisotropic displacement parameters by the full-matrix least-squares technique and hydrogen atoms with isotropic displacement parameters set to 1.2 times of the values for the associated heavier atoms. Detailed information about the crystal data and structure determination are summarized in Table 1. Selected interatomic distances and bond angles are tabulated in Tables 2–4.

Supplementary material for structures **I**–**III** has been deposited with the Cambridge Crystallographic Data Centre (830324 (**I**), 830325 (**II**), and 830326 (**III**); deposit@ccdc.cam.ac.uk or http://www.ccdc.cam.ac.uk).

RESULTS AND DISCUSSION

The asymmetric unit of **I** consists of one Cu^{2+} cation, one Dpds ligand, one 2-MGA anion, and one aqua ligand. As depicted in Fig. 1, the copper ion is located in a CuN_2O_3 square pyramidal coordination environment. The basal plane of Cu atom is defined by one N atom of Dpds ligand, an aqua ligand and two O atoms of *R*- and *S*-methylglutarate anions, respectively with Cu–N/O 1.959–2.038 Å, and the axial position is occupied by N(1) atom of Dpds ligand with Cu–N 2.304 Å. The τ (Addison) value of 0.002 (τ = 0 indicates ideal square pyramidal environment and τ = 1 indicates ideal trigonal bipyramidal enviroment) indicates no significant distortion of the geometry [20]. The Dpds molecule acts as a bis-monodentate bridging ligand with the C–S–S–C torsion angle of 82.69(2)° and the dihedral angles of 85.07(3)° between two pyridyl rings, and the *R*- and *S*-methylglutarato

Table 1. Crystal data and refinement details for structures **I**–**III**

Parameter	Value		
	I	**II**	**III**
Formula weight	444.98	452.32	497.33
Crystal system	*C*2/*c*	*Pc*	*C*2/*c*
Space group	Monoclinic	Monoclinic	Monoclinic
a, Å	18.597(4)	9.538(2)	18.811(4)
b, Å	13.481(3)	10.356(2)	13.482(3)
c, Å	15.126(2)	11.205(2)	15.617(3)
β, deg	104.42(3)	110.54(3)	106.18(3)
Volume, Å	3672.8(1)	1036.4(3)	3803.8(1)
Z	8	2	8
F(000)	1824	465	1988
ρ_{calcd}, g cm^{-3}	1.609	1.449	1.737
Crystal size, mm	0.19 × 0.18 × 0.10	0.49 × 0.21 × 0.13	0.28 × 0.28 × 0.22
μ, cm^{-1}	1.446	1.414	1.398
θ Range for data collection, deg	3.02–27.48	3.12–27.48	3.01–27.47
Index ranges	$-24 \le h \le 24$, $-17 \le k \le 17$, $-19 \le l \le 19$	$-12 \le h \le 12$, $-13 \le k \le 13$, $-14 \le l \le 12$	$-24 \le h \le 18$, $-17 \le k \le 17$, $-20 \le l \le 19$
Measured reflections	17738	10040	18367
Independent reflections (R_{int})	4193 (0.0764)	4229 (0.0553)	4344 (0.0230)
Observed data, $I > 2\sigma(I)$	2587	2570	3644
Parameters	244	247	242
GOOF straight F^2	1.043	1.015	1.038
wR_2 (all data)	0.1634	0.2026	0.1172
R_1 ($I > 2\sigma(I)$)	0.0630	0.0619	0.0410
Largest diff. peak and hole, e/Å^3	1.109 and –0.766	0.941 and –0.300	0.973 and –0.938

Table 2. Selected bond lengths and bond angles with standard deviations in parentheses for **I***

Bond	*d*, Å	Bond	*d*, Å	Bond	*d*, Å
Cu–O(l) Cu–0(4)$^{\#1}$	1.961(4) 1.959(4)	Cu–O(5) Cu–N(l)	1.987(4) 2.304(4)	Cu–N(2)$^{\#2}$	2.038(3)
Angle	ω, deg	Angle	ω, deg	Angle	ω, deg
O(l)CuO(4)$^{\#1}$ O(l)CuO(5) O(l)CuN(l) O(l)CuN(2)$^{\#2}$	172.3(2) 85.9(2) 91.0(2) 91.8(2)	O(4)$^{\#1}$CuO(5) O(4)$^{\#1}$CuN(l) O(4)$^{\#1}$CuN(2)$^{\#2}$ O(5)CuN(l)	86.5(2) 91.0(2) 95.6(2) 95.0(2)	O(5)CuN(2)$^{\#2}$ N(l)CuN(2)$^{\#2}$	172.2(2) 92.5(2)

O–H···O	Distances, Å			O–H···O angle, deg
	O···O	O–H	H···O	
O(5)–H(*w*5*A*)···O(3)	2.664(3)	0.85	1.82	176
O(5)–H(*w*5*B*)···O(2)$^{\#1}$	2.648(2)	0.84	1.81	175

* Symmetry transformations used to generate equivalent atoms: $^{\#1}$ $0.5 - x, 0.5 - y, -z$; $^{\#2}$ $0.5 - x, 0.5 - y, 1 - z$.

Table 3. Selected bond lengths and bond angles with standard deviations in parentheses for **II***

Bond	*d*, Å	Bond	*d*, Å	Bond	*d*, Å
Zn–O(l) Zn–O(3)$^{\#1}$	1.936(9) 1.934(12)	Zn–N(l)	2.011(11)	Zn–N(2)$^{\#2}$	2.057(9)
Angle	ω, deg	Angle	ω, deg	Angle	ω, deg
O(l)ZnO(3)$^{\#1}$ O(l)ZnN(l)	99.5(3) 114.1(4)	O(l)ZnN(2)$^{\#2}$ O(3)$^{\#1}$ZnN(l)	101.8(5) 111.7(4)	O(3)$^{\#1}$ZnN(2)$^{\#2}$ N(l)ZnN(2)$^{\#2}$	112.4(5) 107.7(2)

* Symmetry transformations used to generate equivalent atoms: $^{\#1}$ $x + 1, y, z$; $^{\#2}$ $x, y, z + 1$.

Table 4. Selected bond lengths and bond angles with standard deviations in parentheses for **III***

Bond	*d*, Å	Bond	*d*, Å	Bond	*d*, Å
Cd–O(l) Cd–O(2) Cd–O(3)$^{\#1}$	2.384(5) 2.496(4) 2.678(3)	Cd–O(4)$^{\#1}$ Cd–O(5) Cd–N(l)	2.304(3) 2.322(3) 2.366(3)	Cd–N(2)$^{\#2}$	2.335(3)
Angle	ω, deg	Angle	ω, deg	Angle	ω, deg
O(l)CdO(2) O(1)CdO(3)$^{\#1}$ O(l)CdO(4)$^{\#1}$ O(l)CdO(5) O(l)CdN(l) O(l)CdN(2)$^{\#1}$ O(l)CdO(3)$^{\#1}$	52.5(1) 138.0(1) 162.1(1) 83.1(1) 84.1(1) 107.3(1) 88.3(1)	O(2)CdO(4)$^{\#1}$ O(2)CdO(5) O(2)CdN(l) O(2)CdN(2)$^{\#2}$ O(3)$^{\#1}$CdO(4)$^{\#1}$ O(3)$^{\#1}$CdO(5) O(3)$^{\#1}$CdN(l)	139.2(1) 92.3(1) 135.1(1) 91.8(1) 60.0(1) 84.4(1) 136.7(1)	O(3)$^{\#1}$CdN(2)$^{\#2}$ O(4)$^{\#1}$CdO(5) O(4)$^{\#1}$CdN(l) O(4)$^{\#1}$CdN(2)$^{\#2}$ O(5)CdN(l) O(5)CdN(2)$^{\#2}$ N(l)CdN(2)$^{\#2}$	85.7(1) 82.9(1) 85.8(1) 87.4(1) 93.5(1) 169.2(1) 90.7(1)

O–H···O	Distances, Å			O–H···O angle, deg
	O···O	O–H	H···O	
O(5)–H(5*A*)···O(3)	2.688(2)	0.83	1.87	168
O(5)–H(5*B*)···O(2)$^{\#1}$	2.778(2)	0.82	2.00	159
O(6)–H(6)···O(1)	3.114(2)	0.82	2.37	150

* Symmetry transformations used to generate equivalent atoms: $^{\#1}$ $-x + 0.5, -y + 1.5, -z$; $^{\#2}$ $-x + 0.5, -y + 1.5, -z + 1$.

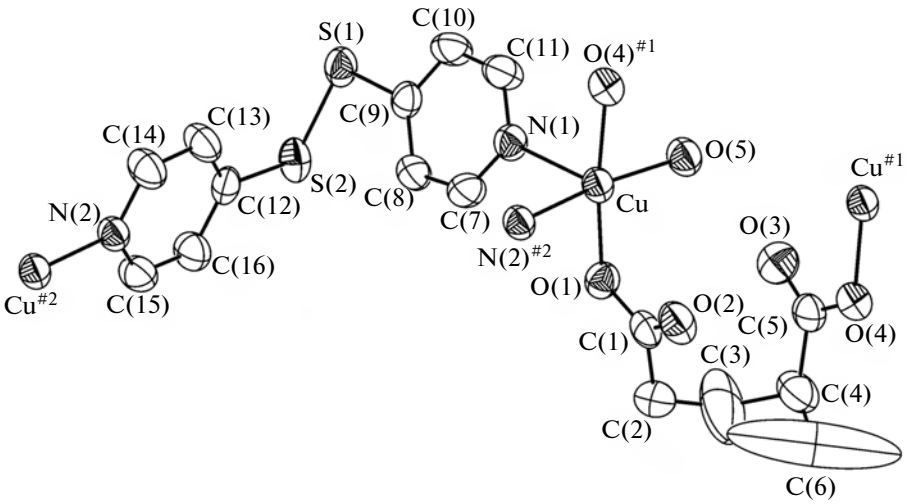

Fig. 1. ORTEP drawing of **I** with ellipsoids at 45% probability level, hydrogen atoms were omitted for clarity.

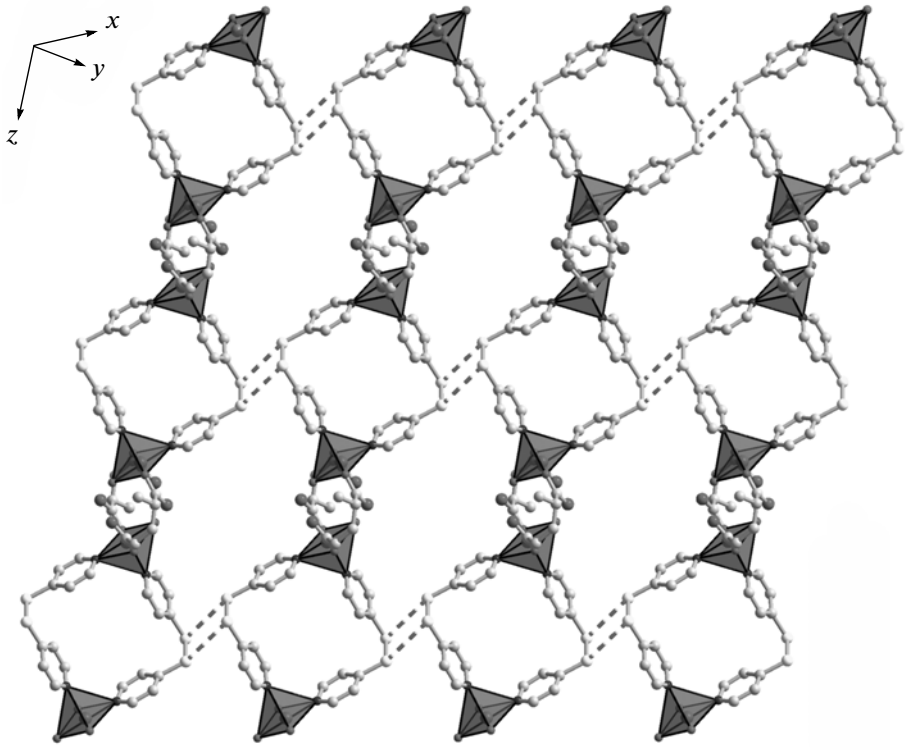

Fig. 2. 2D layer in **I** (dotted lines represent the S···S interactions).

anions display bis-monodentate bridging fashions. The Cu atoms are alternately bridged by Dpds ligands and *R*- and *S*-methylglutarato ligands to generate 1D repeated rhomboids propagating in the [001] direction, and the Cu···Cu separation through Dpds ligand and 2-MGA ligand are 10.371 and 4.835 Å, respectively. Along [110] directions, the adjacent repeated rhomboids are interlinked via S···S weak interactions (S···S distance: 3.638 Å) into 2D layer (Fig. 2). Topologically, the dinuclear unit which was linked by *R*- and *S*-2-methylglutarate ligands was acted as four-connected node, and the Dpds molecule are via the

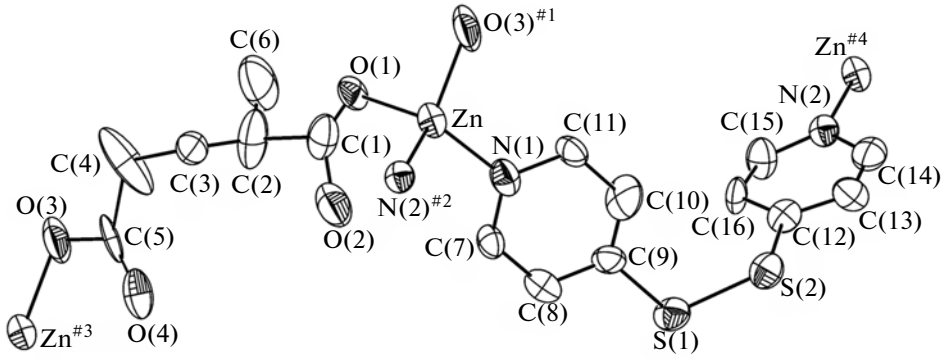

Fig. 3. ORTEP view of coordination environments around Zn with the atom labelling for **II** with ellipsoids at 45% probability (hydrogen atoms were omitted for clarity).

interlayer S···S weak interactions to form the di-Dpds unit, which is defined as four-connected nodes to four dinuclear Cu units. Hence the 2D layer is described as a 2D (4,4) sheet. Because the Cu···Cu separation are 10.371 and 4.835 Å, respectively, the (4,4) nets have enough empty space to provide for interpenetration. The 2D sheets are inclined parallel into 3D network with an inclined angle of 75.5(1)°, to the best of our knowledge, such a inclined (4,4) interpenetration structure has been defined the "2D parallel/2D parallel" mode [21].

The asymmetric unit of **II** contains one Zn^{2+} cation, one Dpds ligand, one 2-MGA anion and one and a quarter lattice water molecule. As shown in Fig. 3, the Zn atoms are each in a distorted tetrahedral coordination sphere defined by two N atoms of two Dpds ligands and two carboxylate O atoms of two MGA anions. The Zn–O/N bond distances range from 1.934(12) to 2.057(9) Å, and the values about the Zn atoms are all within the normal ranges. Similar to **I**, the Dpds ligand acts as a bis-monodentate bridging ligand with the C–S–S–C torsion angle of 94.09(2)° and the dihedral angles of 83.66(2)° between two pyridyl rings. Each carboxylate group of *R*-2-MGA anion in complex **II** coordinates one metal ion, and in this sense, the *R*-2-MGA ligand also function as a bis-monodentate ligand. The Zn atoms are bridged by *R*-2-MGA anion to form 1D chain extending in the [100] direction, which are interconnected by the Dpds ligands to form 2D (4,4) networks as demonstrated in Fig. 4a. The lattice H_2O molecules reside in cavities in the 3D supramolecular architecture (Fig. 4b), which form hydrogen bonds to the carboxylate O atoms as well as to the lattice H_2O molecules.

Within the asymmetric unit of **III** exists one Cd^{2+} cation, one Dpds ligand, a 2-MGA anion, an aqua ligand and a quarter lattice water molecule. Similar to the compound **I** and **II**, the Dpds ligand functions as a bis-monodentate bridging ligand (Fig. 5), and the C–S–S–C torsion angle is 83.46(2)° and the dihedral angles is 85.24(1)° between two pyridyl rings. Different from compounds **I** and **II**, the *R*- and *S*-2-methylglutarate anions are twisted with the terminal carboxylate groups in a chelating fashions. The Cd atoms are each coordinated by two Dpds, one *R*-2-MGA anion, one *S*-2-MGA anion and one aqua ligand to complete a distorted pentagonal bipyramid CdN_2O_4 geometry. The Cd–N/O distance of 2.304–2.678 Å fall in a normal region. The bond angles range from 52.5(1)° to 169.2(1)°, indicating considerable deviation from the regular pentagonal bipyramid. Two Cd atoms bridged *R*- and *S*-2-methylglutarate anions to form a centrosymmetric binuclear complex unit with a rhombus ring, and the binuclear units are connected by Dpds to form 1D repeated rhomboids chain formulated as $^{1}_{\infty}$[Cd(H_2O)(Dpds)(2-MGA)] in the [001] direction. The resulting chains are interlinked via S···S weak interactions (S···S 3.707 Å) into 2D layer (Fig. 6). The 2D sheets are inclined parallel into 3D network, similar to the compound **I**. The lattice H_2O molecules reside in cavities in the 3D supramolecular architecture, which form extensively hydrogen bonds with carboxylate O atoms.

The infrared spectra of complexes **I** and **III** show characteristic broad bands centered at 3165 and 3383 cm^{-1}, respectively, due to the absorption from OH stretching vibration of water molecules in agreement with the X-ray crystallographic analyses described above. The strong sharp absorptions at 1608 cm^{-1} for **I** and 1578 cm^{-1} for **III**, result from antisymmetric stretching (ν_{as}) of the carboxylate groups in 2-MGA anion, and symmetric stretching (ν_s) of the carboxylate groups cause strong sharp absorptions at 1416 cm^{-1} for **I** and 1410 cm^{-1} for **III**, respectively. The Dpds ligand, due to its pyridyl C–H stretching vibrations, causes weak absorptions at 3048 cm^{-1} for **I** and 3058 cm^{-1} for **III**, and the out-of-plane bending vibrations of the pyridyl C–H bonds yield sharp peaks of medium intensities at 716 cm^{-1} for **I** and 710 cm^{-1} for **III**.

(a)

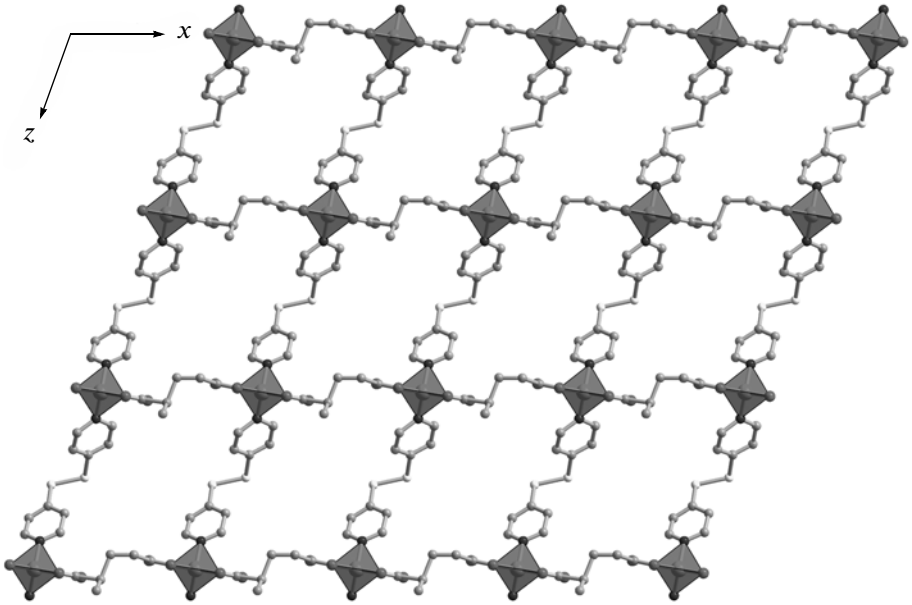

(b)

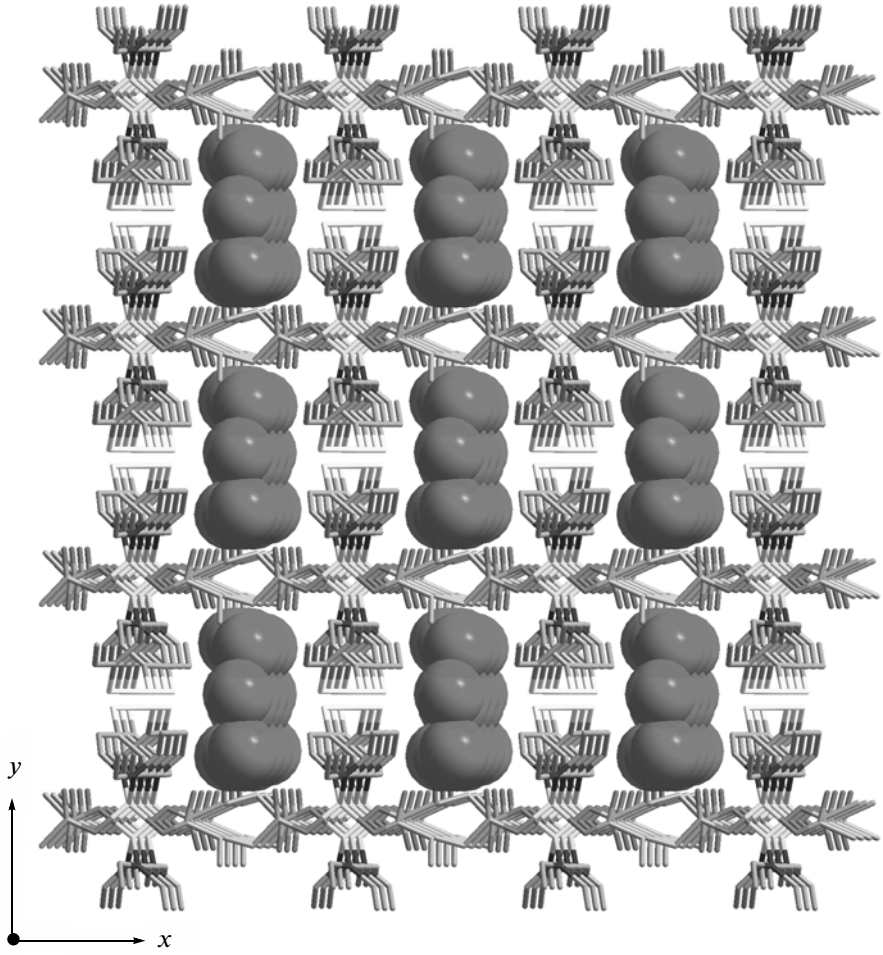

Fig. 4. 2D layer generated from the Zn atoms bridged by 2-MGA anions and Dpds ligands in **II** (a); supramolecular assembly of the 2D layers into 3D architecture (b).

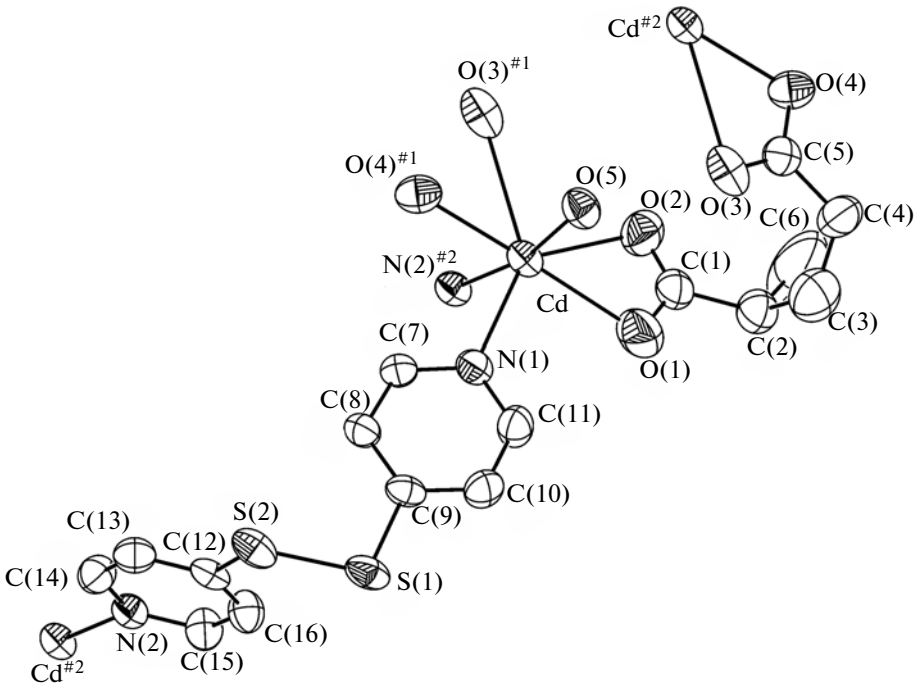

Fig. 5. ORTEP view of coordination environment of Cd ions, 2-MGA anion and Dpds ligand with displacement ellipsoids (45% probability) and atomic labeling in **III** (hydrogen atoms were omitted for clarity).

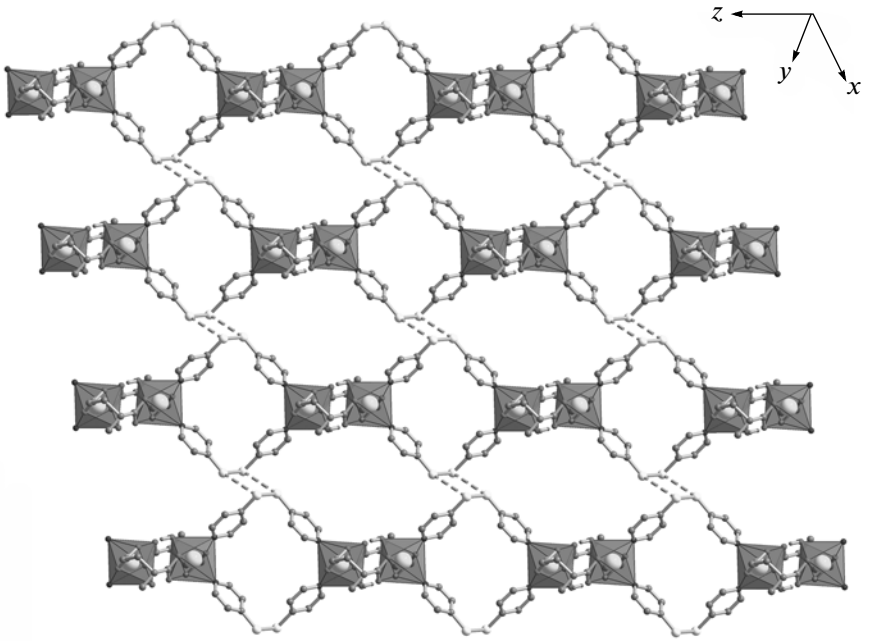

Fig. 6. Supramolecular assembly of 2D layer through S···S interactions in **III**.

The magnetic behavior of compound **I** is depicted in Fig. 7 in the form of χ_m and χ_m^{-1} versus T with χ_m and χ_m^{-1} being the molar magnetic susceptibility and reciprocal molar magnetic susceptibility per Cu^{2+} ion, respectively, and T the temperature. Over the temperature range 2–300 K, the paramagnetic compound **I** obey Curie–Weiss law $\chi_m(T - \theta) = 1.72(9)$ cm^3 K mol^{-1}

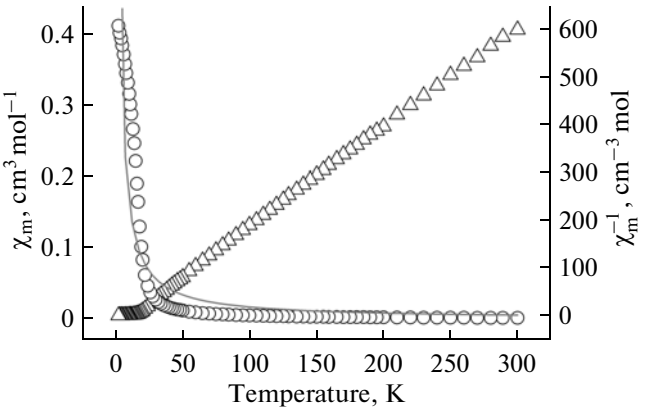

Fig. 7. Temperature dependence of the magnetic susceptibilities of **I** (χ_m being the magnetic susceptibility per one metal ion for **I**). Solid lines represent the best fits.

with the Weiss constant $\theta = -0.50(1)$ K. At room temperature, the effective magnetic moments for compound **I** is 2.00 μ_B, which is larger than the spin-only value of 1.73 μ_B expected for one unpaired electron of Cu^{2+} ion with d^9 configuration [22].

ACKNOWLEDGMENTS

This project was supported by the Scientific Research Fund of Ningbo University (grants nos. XKL11058 and XYL11005) and K.C. Wong Magna Fund in Ningbo University.

REFERENCES

1. Kitagawa, S., Kitaura, R., Noro, S.I., et al., *Angew. Chem. Int. Ed.*, 2004, vol. 43, p. 2334.
2. Fujita, M., Kwon, Y.J., Washizu, S., et al., *J. Am. Chem. Soc.*, 1994, vol. 116, p. 1151.
3. Evans, O.R. and Lin, W., *Acc. Chem. Res.*, 2002, vol. 35, p. 511.
4. Kahn, O., *Acc. Chem. Res.,* 2000, vol. 33, p. 647.
5. Froster, M.P. and Cheetham, A.K., *Angew. Chem. Int. Ed.*, 2002, vol. 41, p. 457.
6. Konar, S., Zangrando, E., Drew, M.G.B., et al., *Dalton Trans.*, 2004, p. 260.
7. Horikoshi, T. and Mochida, T., *Coord. Chem. Rev.*, 2006, vol. 250, p. 2595.
8. Suen, M.C., Wang, Y.H., Hsu, Y.F., et al., *Polyhedron*, 2005, vol. 24, p. 2913.
9. Marinho, M.V., Yoshida, M.I., Krambrock, K., et al., *J. Mol. Struct.*, 2009, vol. 923, p. 60.
10. Lu, J.F., Xu, Q., Zhou, Q.X., et al., *Inorg. Chim. Acta*, 2009, vol. 362, p. 3401.
11. Ma, L.F., Wang, L.Y., Hu, J.L., et al., *CrystEngComm*, 2009, vol. 11, p. 777.
12. Zheng, Y.-Q., Lin, J.L., and Kong, Z.P., *Inorg. Chem.*, 2004, vol. 43, p. 2590.
13. Zheng, Y.-Q., Lin, J.L., Xu, W., et al., *Inorg. Chem.*, 2008, vol. 47, p. 10280.
14. Zheng, Y.-Q., Cheng, D.Y., Lin, J.L., et al., *Eur. J. Inorg. Chem.*, 2008, p. 4453.
15. Delgado, L.C., Fabelo, O., Pasan, J., et al., *Inorg. Chem.*, 2007, vol. 46, p. 7458.
16. Chen, B., Ji, Y., Xue, M., et al., *Inorg. Chem.*, 2008, vol. 47, p. 5543.
17. Zheng, Y.-Q., Liu, W., and Yao, F.Y., *J. Coord. Chem.*, 2009, vol. 62, p. 2497.
18. Livage, C., Guillou, N., Rabu, P., et al., *Chem. Commun.*, 2009, p. 4551.
19. Sheldrick, G.M., *SHELXS-97, Program for Crystal Stucture Refinement and SHELXL-97, Program for Crystal Stucture Solution*, Göttingen (Germany): Univ. of Göttingen, 1997.
20. Addison, A.W. and Rao, N., *Dalton Trans.*, 1984, p. 1349.
21. Batten, S.R., Neville, S.M., and Turner, D.R., *Coordination Polymers Design, Analysis and Application*, UK: RSC, 2009.
22. Boudreaux, E.A. and Mulay, L.N., *Theory and Applications of Molecular Paramagnetism*, New York: Wiley, 1976.